Interferometric frequency-resolved optical gating

Gero Stibenz and Günter Steinmeyer

Max-Born-Institute for Nonlinear Optics and Short Pulse Spectroscopy, Max-Born-Straße 2a, 12489 Berlin, Germany

stibenz@mbi-berlin.de

Abstract: We demonstrate a novel variant of frequency-resolved optical gating (FROG) that is based on spectrally resolving a collinear interferometric autocorrelation rather than a noncollinear one. From the interferometric FROG trace, one can extract two terms, the standard SHG-FROG trace and a new phase-sensitive modulational component, which both allow for independent retrieval of the pulse shape. We compare the results of both methods and a separate SPIDER measurement using 6.5-fs pulses from a white-light continuum. We find that the novel modulational component allows for robust retrieval of pulse shapes in the few-cycle regime. Together with the added cross-checks, our method significantly enhances choices for pulse characterization in this regime.

© 2005 Optical Society of America

OCIS codes: 320.5520 (pulse compression), 320.7100 (ultrafast measurements), 320.7160 (ultrafast technology)

References and links

1. J.-C. Diels, E. Van Stryland, and G. Benedict, "Generation and measurement of 200 femtosecond optical pulses," Opt. Commun. **25**, 93-95 (1978).
2. J.-C. Diels and W. Rudolph, "Ultrashort Laser Pulse Phenomena," Academic Press, San Diego, CA (1996).
3. K. Naganuma, K. Mogi, and H. Yamada, "General Method for Ultrashort Light Pulse Chirp Measurement," IEEE J. Quantum Electron. **25,** 1225-1233 (1989).
4. J.-H. Chung, and A. M. Weiner, "Ambiguity of Ultrashort Pulse Shapes Retrieved From the Intensity Autocorrelation and the Power Spectrum," IEEE J. Sel. Top. Quantum Electron. **7,** 656-666 (2001).
5. R. Trebino, K. W. De Long, D. N. Fittinghoff, J. N. Sweetser, M. A. Krumbügel, B. A. Richman, and D. J. Kane, "Measuring ultrashort laser pulses in the time-frequency domain using frequency-resolved optical gating," Rev. Sci. Instrum. **68**, 3277-3295 (1997).
6. R. Trebino, "Frequency-Resolved Optical Gating: The Measurement of Ultrashort Laser Pulses," Kluwer Academic Publishers, Boston, MA (2000).
7. C. Iaconis and I. A. Walmsley, "Spectral phase interferometry for direct electric-field reconstruction of ultrashort optical pulses," Opt. Lett. **23,** 792-794 (1998).
8. C. Iaconis and I. A. Walmsley, "Self-referencing spectral interferometry for measuring ultrashort optical pulses," IEEE J. Quantum Electron. **35,** 501-509 (1999).
9. A. Baltuška, M. S. Pshenichnikov, and D. A. Wiersma "Amplitude and phase characterization of 4.5-fs pulses by frequency-resolved optical gating," Opt. Lett. **23**, 1474-1476 (1998).
10. L. Gallmann, D. H. Sutter, N. Matuschek, G. Steinmeyer, U. Keller, C. Iaconis, and I. A. Walmsley, "Characterization of sub-6-fs optical pulses with spectral phase interferometry for direct-field reconstruction," Opt. Lett. **24,** 1314-1316 (1999).
11. A. Baltuška, T. Fuji, and T. Kobayashi, "Visible pulse compression to 4 fs by optical parametric amplification and programmable dispersion control," Opt. Lett. **27**, 306-308 (2002).
12. K. Yamane, Z. G. Zhang, K. Oka, R. Morita, M. Yamashita, and A. Suguro, "Optical pulse compression to 3.4 fs in the monocycle region by feedback phase compensation," Opt. Lett. **28**, 2258-2260 (2003).
13. F. Reynaud, F. Salin, and A. Barthelemy, "Measurement of phase shifts introduced by nonlinear optical phenomena on subpicosecond pulses," Opt. Lett. **14**, 275-277 (1989).

#6789 - $15.00 US Received 8 March 2005; revised 22 March 2005; accepted 22 March 2005

14. A. Baltuška, Z. Wei, M. S. Pshenichnikov, and R. Szipőcs, "All-solid-state cavity-dumped sub-5-fs laser," Appl. Phys. B **65**, 175-188 (1997).
15. I. A. Roldán, I. G. Cormack, P. Loza-Alvarez, E. J. Gualda, and D. Artigas, "Ultrashort pulse characterization with SHG collinear-FROG," Opt. Express **12,** 1169–1178 (2004), http://www.opticsexpress.org/abstract.cfm?URI=OPEX-12-6-1169.
16. Certain commercial instruments and software packages are identified in this paper only to facilitate experimental reproducibility and to adequately describe the experimental procedure. Such identification does not imply any recommendation, nor does it imply that the equipment identified are necessarily the best available for the purpose.
17. G. Sansone, G. Steinmeyer, C. Vozzi, S. Stagira, M. Nisoli, S. De Silvestri, K. Starke, D. Ristau, B. Schenkel, J. Biegert, A. Gosteva, and U. Keller, "Mirror dispersion control of a hollow fiber supercontinuum," Appl. Phys. B, **78**, 551-555, (2004).
18. L. Cohen, "Time-frequency distributions - a review," Proc. IEEE **77**, 941-981 (1989).
19. FROG software Ver. 3.0, http://www.femtosoft.biz/
20. M. Takeda, H. Ina, and S. Kobayashi, "Fourier-transform method of fringe-pattern analysis for computer-based topography and interferometry," J. Opt. Soc. Am. **72,** 156 (1982).
21. K. W. DeLong, D. N. Fittinghoff,R. Trebino,B. Kohler, and K. Wilson, "Pulse Retrieval in Frequency-Resolved Optical Gating Based on the Method of Generalized Projections," Opt. Lett. **19,** 2152–2154 (1994).
22. D. T. Reid, "Algorithm for complete and rapid retrieval of ultrashort pulse amplitude and phase from a sonogram," IEEE J. Quant. El. **35,** 1584–1589 (1999).
23. W. H. Press, S. A. Teukolsky, W. T. Vetterlin, and B. P. Flannery, "Numerical Recipes in C,", 2nd ed., ch. 10.5, pp. 412, Cambridge University Press, Cambridge, UK, 1992.
24. G. Stibenz and G. Steinmeyer, "High dynamic range characterization of ultra-broadband white-light continuum pulses," Opt. Express **12,** 6319–6325 (2004), http://www.opticsexpress.org/abstract.cfm?URI=OPEX-12-25-6319.

1. Introduction

The development of measurement methods that reveal both, the amplitude and the phase structure of a short pulse, has significantly enhanced the possibilities of characterizing ultrashort laser pulses. These complete characterization methods have now widely replaced interferometric autocorrelation (IAC) [1, 2], in particular for measurement of sub-10-fs pulses. An early attempt to retrieve the pulse shape and phase from an IAC with the added information on the first-order correlation or spectrum of the pulse has been described by Naganuma et al. [3]. However, it was shown recently that unambiguous retrieval is experimentally challenging as different pulse shapes with equal power spectrum may display practically indistinguishable interferometric autocorrelation traces [4]. Pulse shape and phase become accessible, though, when spectrally resolving the autocorrelation, which results in measurement of a two-dimensional rather than that of two one-dimensional data traces. This complete characterization method has been termed frequency-resolved optical gating (FROG [5, 6]). Almost all recent reports on record-breaking pulse durations have either been based on FROG or on an alternative complete method called spectral phase interferometry for direct-electric field reconstruction (SPIDER, [7, 8]), see e.g. [9–12].

Both techniques have their specific strengths. Being a variant of spectral interferometry [13], SPIDER is particularly suited for measurements of the spectral phase of a pulse, which is advantageous for tracking the influence of dispersion on a short pulse. FROG, on the other hand, retrieves the electric field of a pulse iteratively from a spectrally resolved autocorrelation. Therefore FROG appears better suited for resolving the exact satellite structure of a complicated pulse, whereas it can only indirectly reconstruct its spectral phase. Often it would be desirable to have a technique at hand that combines both, a direct phase sensitivity and a sensitivity on the temporal envelope structure of the pulse.

When measuring pulses in the few-cycle regime, both techniques require special care because of the enormous bandwidths involved and the often observed complex spectro-temporal structures of the pulses. Additionally, standard second harmonic FROG, as a noncollinear technique, can be corrupted by geometrical smearing of the pulse structure due to the finite crossing

#6789 - $15.00 US Received 8 March 2005; revised 22 March 2005; accepted 22 March 2005
(C) 2005 OSA

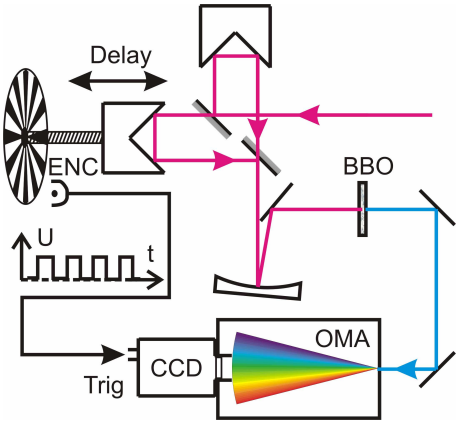

Fig. 1. Experimental arrangement of a dispersion balanced interferometric autocorrelator. Spectrally resolving the autocorrelation signal results in an interferometric FROG trace (See Fig. 2). The fringe substructure of the IFROG trace is preserved by triggering a fast camera with the encoder signal of a constant moving delay stage. ENC, encoder; OMA, optical multichannel analyzer.

angle of the beams [6, 14]. This has to be carefully avoided when using this technique in the few-cycle regime. Recently, it has been suggested to extract the second harmonic FROG trace from an interferometric FROG measurement with collinear beams [15]. While the information from the interferometric modulation of those FROG traces was discarded in this first demonstration, we will show how to use this information to independently reconstruct the pulse shape. Alternatively, this information can be used as an additional cross check, which is particularly valuable for the measurement of few-cycle pulses.

2. Experimental set-up

At first sight, it appears straightforward to spectrally resolve an interferometric autocorrelation trace and to develop this method into a novel kind of FROG. There are, however, two major problems that have hindered this approach so far. First, it is necessary to sample spectra at sub-wavelength delay steps without corruption due to interferometer drift. Second, this dense sampling of the FROG trace results in an overwhelming amount of data, which causes slow convergence during reconstruction or may even prevent any meaningful interpretation of the data. In the following we present a solution for both these technical problems.

Rather than actively stabilizing our interferometer we choose to decrease the measurement time to the minimum amount possible, utilizing a fast line-scan camera capable of kHz acquisition of spectra (Dalsa CL-C6 2048T [16]). To improve the signal-to-noise ratio of the data, we averaged 10 independent scans of our FROG trace. To synchronize acquisition of spectra, the camera is directly triggered by the chopper wheel encoder of a conventional crossed-roller bearing translation stage (Physik Instrumente M126.D [16]), see Fig. 1. The delay stage moves at constant speed throughout the entire measurement window, triggering camera shots at a rate of 100 Hz on the fly. This way, a delay range of 100 fs is equidistantly sampled in only 5 seconds, which corresponds to about 30 ms per fringe of the fundamental wavelength. Spectra are sampled at a delay step of 225 attoseconds, i.e., $1/12$ wave at 800 nm. Regarding the second harmonic, data is sampled at about 3 times the Nyquist limit.

We use a standard dispersion balanced collinear interferometer with two broadband (440-

#6789 - $15.00 US
Received 8 March 2005; revised 22 March 2005; accepted 22 March 2005
(C) 2005 OSA

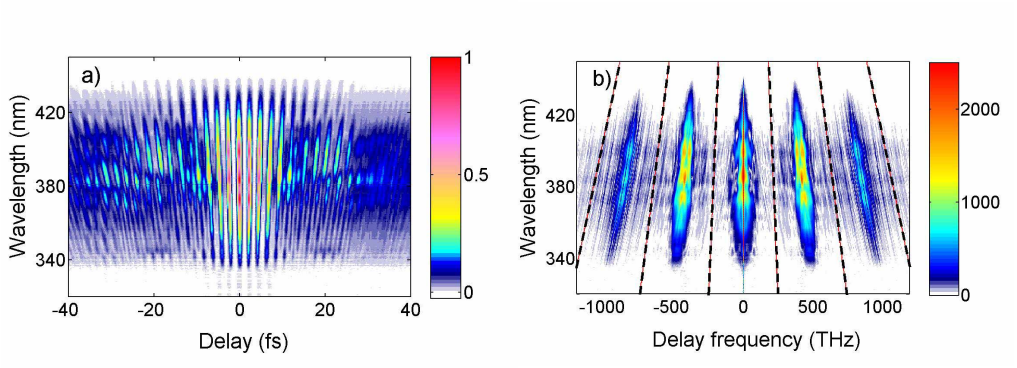

Fig. 2. Interferometric FROG. (a) Spectrally resolved interferometric autocorrelation (IFROG) trace. (b) Fourier transform of (a) along the delay axis. The dc baseband, two modulation side bands at the fundamental frequency ω_0, and two second harmonic side bands (at $2\omega_0$) are clearly separable. The dashed lines mark the borders of a super-Gaussian filter that was used for isolating the individual components.

1040 nm) 1-mm thick beamsplitters. We employ a convex mirror with 30 cm focal length for focusing the beam into a 10μm thick β-BaB_2O_4 (BBO) crystal. Figure 2(a) shows an example of a spectrally resolved interferometric autocorrelation, i.e., an interferometric FROG (IFROG) measurement. This measurement is based on 7-fs pulses from a white-light continuum, which cover a bandwidth of about 300 nm. The pulses were generated by focusing 700-μJ pulses from a 30-fs Ti:sapphire amplifier into a 250 μm diameter hollow capillary filled with 400 mbar of argon gas and subsequent compression with chirped mirrors [17].

For further analysis, we Fourier transform the IFROG trace along the delay axis, see Fig. 2(b). In this representation one can clearly distinguish the dc baseband and four modulational side bands, two of which correspond to the fundamental frequency and two to the second harmonic (SH). The sharpness of the SH lines in Fig. 2(b) is a measure for the uniformity of the movement of the translation stage. In fact, one can extract a measure for the rms phase jitter of the SH sidebands from this trace of about 1 rad. This jitter can be related to an average positioning error of the stage of only 0.2 fs, which is of the order of the step width. Such a high resolution can only be achieved because the measurement is carried out on the fly, rather than in a stepwise approach with frequent stopping and repositioning of the stage. In particular, there are no indications for cycle slip artifacts, i.e. phase jumps of $> 2\pi$ that would corrupt the IFROG trace. Outside the relevant delay window, several minor phase jumps appear at certain wavelengths. These discontinuities can be removed by phase unwrapping.

3. Structure of the IFROG trace

For a full understanding of the structure of the IFROG trace and to find an analytical expression for the side bands in the Fourier domain [Fig. 2(b)] one has to Fourier-transform the second harmonic of two pulses with a relative delay of τ. Each pulse is described by a complex electric field

$$\mathscr{E}(t) = E(t)\exp(i\omega_0 t) \tag{1}$$

with the complex amplitude $E(t)$ and the carrier angular-frequency ω_0. The measured intensity of the interferometric FROG signal can then be written as [15]

$$I_{\mathrm{IFROG}}(\omega,\tau) = \left| \int_{-\infty}^{\infty} (\mathscr{E}(t) + \mathscr{E}(t-\tau))^2 \exp(-i\omega t)\, \mathrm{d}t \right|^2 . \tag{2}$$

#6789 - $15.00 US
Received 8 March 2005; revised 22 March 2005; accepted 22 March 2005
(C) 2005 OSA

Substituting $\Delta\omega = \omega - 2\omega_0$ and using the following equations for the standard second harmonic FROG field of the two pulses

$$E_{\mathrm{FROG}}(\Delta\omega,\tau) = \int_{-\infty}^{\infty} E(t)E(t-\tau)\exp(-i\Delta\omega t)\,\mathrm{d}t \tag{3}$$

and for the second harmonic (SH) field of a single pulse

$$E_{\mathrm{SH}}(\Delta\omega) = E_{\mathrm{FROG}}(\Delta\omega,\tau=0) = \int_{-\infty}^{\infty} E^2(t)\exp(-i\Delta\omega t)\,\mathrm{d}t, \tag{4}$$

we can Fourier-transform Eq. (2) and retrieve the following expression for the IFROG trace:

$$I_{\mathrm{IFROG}}(\omega,\tau) = \left|\left(1+\exp(-i(2\omega_0+\Delta\omega)\tau)\right)E_{\mathrm{SH}}(\Delta\omega) + 2\exp(-i\omega_0\tau)\,E_{\mathrm{FROG}}(\Delta\omega,\tau)\right|^2. \tag{5}$$

After expansion we can isolate four terms:

$$\begin{aligned} I_{\mathrm{IFROG}}(\omega,\tau) &= 2\left|E_{\mathrm{SH}}(\Delta\omega)\right|^2 + 4\left|E_{\mathrm{FROG}}(\Delta\omega,\tau)\right|^2 \\ &+ 8\cos\left[\left(\omega_0+\frac{\Delta\omega}{2}\right)\tau\right]\mathrm{Re}\left[E_{\mathrm{FROG}}(\Delta\omega,\tau)E^*_{\mathrm{SH}}(\Delta\omega)\exp\left(i\frac{\Delta\omega}{2}\tau\right)\right] \\ &+ 2\cos\left[(2\omega_0+\Delta\omega)\tau\right]\left|E_{\mathrm{SH}}(\Delta\omega)\right|^2. \end{aligned} \tag{6}$$

The first two terms constitute the unmodulated kernel of the trace and correspond to the baseband of Fig. 2(b). This dc part consists of the standard SH-FROG trace $I_{\mathrm{FROG}}(\omega,\tau) = |E_{\mathrm{FROG}}(\omega,\tau)|^2$ and a delay-independent background $2|E_{SH}(\omega)|^2$. The third term in Eq. (6) is an interferometric contribution, which is modulated at the fundamental periodicity, accounting for the sidebands at $-\omega_0$ and $+\omega_0$ in Fig. 2(b). Notably, this term has a linear dependence on the amplitude of the FROG field E_{FROG}, but also depends on the relative phase between E_{FROG} and the SH field E_{SH}. The last term in Eq. (6), finally, is similar to the SH background of the baseband but appears modulated at the second harmonic of the carrier frequency. This term gives rise to the sidebands around $-2\omega_0$ and $+2\omega_0$ in Fig. 2(b). Together with the first term, this modulation at the second harmonic wavelength can be understood as spectral interferometry between the two SH pulses at a delay τ. At first sight, this term may appear useless for reconstruction of the pulse shape. However, it can be used to provide an intrinsic phase reference with $\varphi_{\mathrm{mod}} = (2\omega_0+\Delta\omega)\tau$ which can be used for phase-sensitive extraction of the $\propto \cos(\varphi_{\mathrm{mod}}/2)$ fundamental interference term. Isolating the SH modulation term also allows for a judgment on the integrity of the observed fringe patterns, as was already discussed above. The components of the IFROG trace can easily be isolated in the experimental data by Fourier filtering, as indicated by the dashed lines in Fig. 2(b). For this purpose we used super-Gaussian filtering.

Let us turn our attention to the fundamental modulation term in Eq. (6), which represents a new kind of FROG trace. In the following, we will refer to this portion of the interferometric FROG trace as fundamental-modulation FROG (FM-FROG). This trace can be written as

$$\begin{aligned} I_{\mathrm{FMFROG}}(\Delta\omega,\tau) &= \left|E_{\mathrm{FROG}}(\Delta\omega,\tau)\right|\left|E_{\mathrm{FROG}}(\Delta\omega,\tau=0)\right| \times \\ &\quad \cos\left(\varphi_{\mathrm{FROG}}(\Delta\omega,\tau) - \varphi_{\mathrm{FROG}}(\Delta\omega,\tau=0) + \frac{\Delta\omega}{2}\tau\right) \end{aligned} \tag{7}$$

The FM-FROG trace has some interesting properties, which sets it apart from any previously described variant of FROG. First and foremost, it is the real part of a product of complex

#6789 - $15.00 US Received 8 March 2005; revised 22 March 2005; accepted 22 March 2005
(C) 2005 OSA

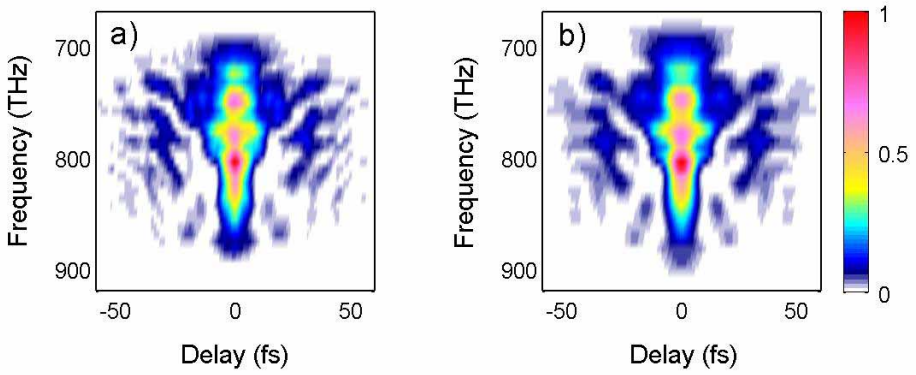

Fig. 3. Pulse retrieval from the dc part of the IFROG trace. (a) SH-FROG trace, as extracted from the IFROG trace. (b) Reconstructed SH-FROG trace. The FROG error of this reconstruction is 0.005. The retrieved temporal and spectral phase and intensity profiles of the pulse are plotted in Fig. 6(c) and (d).

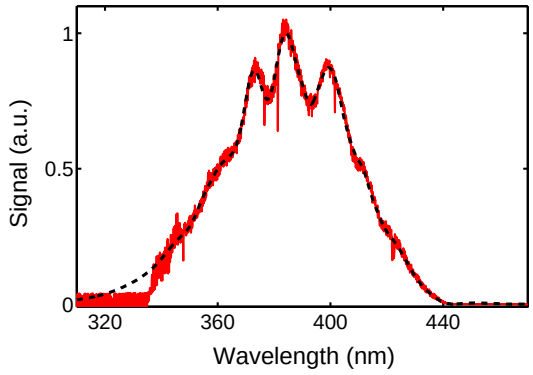

Fig. 4. Red curve: Frequency marginal after compensating the bandwidth limitation of the conversion process. Black dashed line: Convolution of the fundamental pulse spectrum.

numbers and can therefore become negative, very similar to the Wigner trace [18]. Obviously, the sign of the FM-FROG trace is connected to the phase differences in the cosine term of Eq. (7), i.e. there is a direct dependence on phase. For a transform-limited Gaussian pulse $\varphi_{\mathrm{FROG}}(\Delta\omega,\tau=0)$ is a constant, and the remaining FROG phase $\varphi_{\mathrm{FROG}}(\Delta\omega,\tau)$ is almost compensated by the linear phase contribution $\Delta\omega\,\tau/2$. An FM-FROG trace of such a pulse therefore exhibits virtually no negative portions within any reasonable delay window. In contrast, even a small chirp on the pulse causes a noticeable change of $\varphi_{\mathrm{FROG}}(\Delta\omega,\tau)$. It is evident that rapid oscillations of the FM-FROG trace are an indication for a strong chirp on the pulse. However, satellite pulses at larger delays can also give rise to negative portions of the FM-FROG trace, even in the absence of a chirp.

In more practical terms, the FM-FROG trace is also interesting because it is background free, other than the SH-FROG trace embedded in the dc term of Eq. (6). A further incentive for using the FM-FROG trace for pulse retrieval is the linear dependence on $E_{\mathrm{FROG}}(\omega,\tau)$, which ensures a more effective use of the dynamic range of the camera when scanning τ.

#6789 - $15.00 US
Received 8 March 2005; revised 22 March 2005; accepted 22 March 2005
(C) 2005 OSA

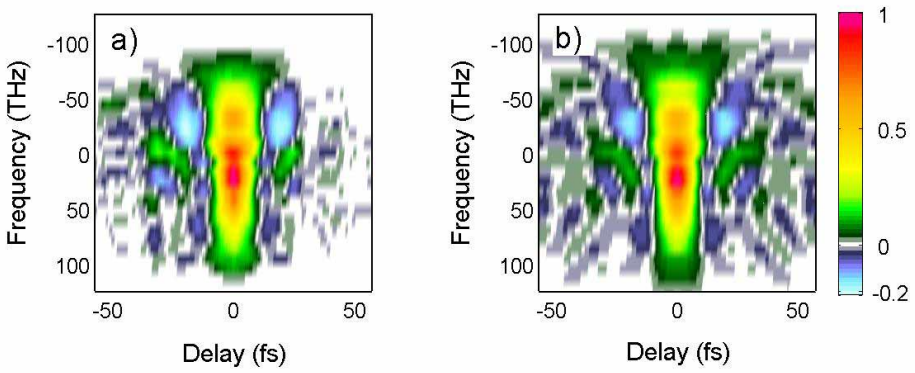

Fig. 5. Pulse retrieval from the ac part of the IFROG trace. (a) FM-FROG trace, i.e. modulated part at the interference period of the fundamental, phase-sensitively extracted from the IFROG data in Fig. 2(a). (b) Reconstructed FM-FROG trace derived by the implementation of a modified generalized projection method for the pulse-retrieval. The FROG error of this reconstruction is 0.0085. The retrieved temporal and spectral phase and intensity profiles of the pulse are plotted in Fig. 6(e) and (f).

4. Pulse retrieval

Because the FROG field is encoded twice in the IFROG trace we can independently retrieve the electric field of the measured pulse in two different ways. The first possibility is extraction of the dc baseband in Fig. 2(b). After an inverse Fourier transform back into the time domain, the background term $2|E_{\mathrm{SH}}(\omega)|^2$ can be isolated at large delays τ and is subtracted from the dc component. As a result of this procedure one obtains the SH FROG trace $|E_{\mathrm{FROG}}(\omega,\tau)|^2$ shown in Fig. 3(a). As this is essentially the same trace as obtained in a noncollinear geometry, one can employ standard FROG algorithms. This procedure is applicable even if the fringe structure of the IFROG trace is washed out or undersampled, as demonstrated in Ref. [15]. We apply a commercial pulse retrieval code [16, 19], which readily converges down to a FROG error of 0.0052 on a 256×256 grid, employing the generalized projection-overstep algorithm. The retrieved pulse has a FWHM duration of 7.4 fs [cf. Fig. 6(c)] and yields the reconstructed FROG trace of Fig. 3(b). We compensated for bandwidth limitations of the SH process in the BBO-crystal and for a spectral dependence of the detection efficiency using the method described in Ref. [14]. The frequency marginal after this correction is displayed in Fig. 4.

The second method for pulse retrieval, extraction of the FM-FROG trace [Eq. (7)] from the IFROG measurement, is more elaborate as it relies on determination of the phase $\varphi_{\mathrm{mod}}(\omega,\tau)$ of the cosine in Eq. (6), i.e., the phase of the SH sidebands. Therefore, this method is only applicable for uncorrupted fringe-resolved IFROG measurements. The modulated SH signal provides marker fringes, which allow for an independent reconstruction of the delay τ and provide a local oscillator for phase-sensitive extraction of the fundamental modulation. The phase of the SH sideband is extracted via Fourier filtering [cf. Fig. 2(b)] with subsequent phase retrieval, similar to the method employed in spectral interferometry [20]. This method yields $\varphi_{\mathrm{mod}}(\omega,\tau)$, which is then used to extract the FM-FROG trace from the measured data. Isolating the fundamental sidebands in Fig. 2(b), transforming back into the time domain and multiplying by $\cos(\varphi_{\mathrm{mod}}/2)$ eliminates the cosine in the second term of Eq. 6 and yields the FM-FROG trace. This phase-sensitive filtering method ensures the correct sign of the FM-FROG trace, which is absolutely mandatory for its interpretation.

Figure 5(a) displays the extracted FM-FROG trace after low pass filtering. Careful compari-

#6789 - $15.00 US Received 8 March 2005; revised 22 March 2005; accepted 22 March 2005
(C) 2005 OSA

son to Fig. 2(a) reveals that negative regions of the FM-FROG trace correspond to regions of the IFROG trace, where the fundamental modulation is in antiphase to the modulation around zero delay, e.g. the surroundings of ($\tau = \pm 20$ fs, $\lambda = 400$ nm). Because of experimental imperfections, the FM-FROG trace exhibits slight deviations from symmetry at larger delays $\tau > 25$ fs. Note that this does not affect reconstruction of the main pulse.

Unfortunately, the FM-FROG signal cannot easily be processed with standard FROG strategies. Most FROG retrieval algorithms, even the simplest ones, require a projection step, which cannot easily be implemented in case of the non-semidefinite FM-FROG trace. Also, it is difficult to define a generic signal field for this kind of FROG trace. Nevertheless, generalizing the retrieval strategies, one can modify the generalized projections algorithm (GPA) [21,22] for the FM-FROG case. The goal of such a strategy is to iteratively minimize the functional distance

$$Z = \sum_{i,j=1}^{N} \left| I^{\mathrm{meas}}_{\mathrm{FMFROG}}(\Delta\omega_i, \tau_j) - I^{(k)}_{\mathrm{FMFROG}}(\Delta\omega_i, \tau_j) \right|^2 . \tag{8}$$

where $I^{\mathrm{meas}}_{\mathrm{FMFROG}}(\Delta\omega_i, \tau_j)$ is the measured FM-FROG data and $I^{(k)}_{\mathrm{FMFROG}}(\Delta\omega_i, \tau_j)$ is the FM-FROG trace calculated for the k-th iteration of the electric field $E^{(k)}(t_i)$. One difference to common FROG retrieval is that Z is evaluated in the frequency-delay domain rather than in the time-delay domain. Instead, Fourier transforms have to be applied to $E^{(k)}(t_i)$ for computing the input data to Eq. (8). Despite these concessions to practical issues of FM-FROG retrieval, the structure of GPA retrieval as a local gradient fitting strategy is conserved. In the modified GPA approach, the next iteration $E^{(k+1)}$ for the pulse field is also found by line minimization [23] along the gradient of Z according to

$$E^{(k+1)}(t_i) = E^{(k)}(t_i) + \mu \left(\frac{\partial Z}{\partial \mathrm{Re}\,[\mathrm{E}(\mathrm{t_i})]} \right) + i\,\mu \left(\frac{\partial Z}{\partial \mathrm{Im}\,[\mathrm{E}(\mathrm{t_i})]} \right) \tag{9}$$

where μ is the factor that minimizes Z along the gradient $(\partial Z/\partial \mathrm{Re}\,[\mathrm{E}(\mathrm{t_i})] + \mathrm{i}\partial \mathrm{Z}/\partial \mathrm{Im}\,[\mathrm{E}(\mathrm{t_i})])$.

We used this strategy to retrieve the electric field directly from the measured FM-FROG data. As a seed for the retrieval algorithm, we either used a Gaussian pulse with a flat phase or, alternatively, the pulse reconstructed from the dc baseband. The minimization procedure seeded with the SH-FROG pulse starts at an FM-FROG error of 0.0122 and converges to a value of 0.0085 within 30 iterations. The resulting pulse has a FWHM-duration of 6.8 fs and is displayed in Fig. 6(e). Figure 5(b) shows the associated, reconstructed FM-FROG trace. Retrieval from scratch with a Gaussian seed delivers very similar results and FROG errors, but requires > 100 iterations. Comparing SH-FROG retrieval [Fig. 6(c)] and FM-FROG retrieval [Fig. 6(e)], one finds that all major characteristics of the measured trace are very well reproduced and that differences between the methods are minor. FM-FROG yields a smaller satellite content and shorter pulse duration, but the retrieved satellite structure is very similar for both methods.

5. Discussion

This situation calls for a third independent measurement of the pulse shape. To check the reliability of the presented pulse retrieval methods we also measured the optical pulses with a SPIDER apparatus, optimized for sub-10 fs pulses [24]. A spectral interferogram directly delivers the spectral phase of the pulse [red curve in Fig. 6(a)]. Along with the independently measured spectral density [black curve in Fig. 6(b)], which was also used for the frequency-marginal check, we compute the temporal intensity and phase structure of the pulse [Fig. 6(a)]. It should be noted that for practical reasons the SPIDER measurement could not be carried out at exactly the same time as the IFROG measurements. This procedure may hold for small discrepancies. However, measures were taken to ensure that both measurements experienced the

#6789 - $15.00 US Received 8 March 2005; revised 22 March 2005; accepted 22 March 2005
(C) 2005 OSA

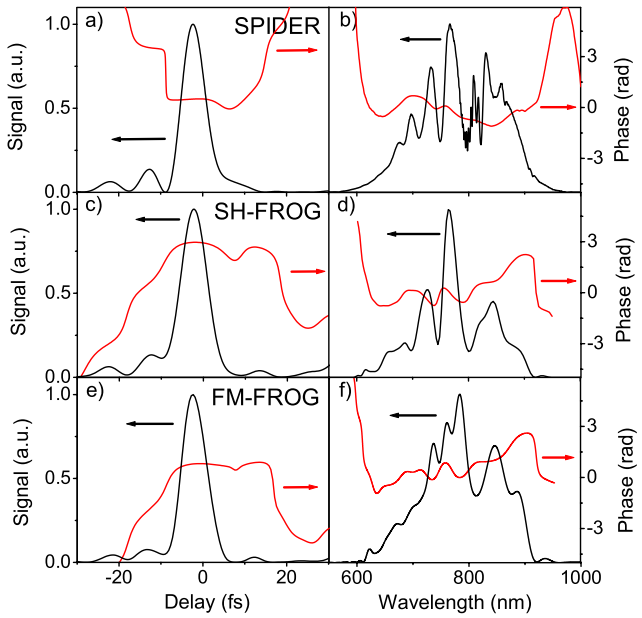

Fig. 6. Comparison of pulse shapes retrieved by SPIDER (a,b), SH-FROG (c,d), and FM-FROG (e,f). Temporal shapes are shown in (a, c, and e), reconstructed spectra are shown in (d) and (f). An independent measurement of the pulse spectrum, which also served for the marginal test, is shown in (b) together with the spectral phase measured in SPIDER. Intensities are shown in black, phases in red. The FWHM pulse durations are: 6.5 fs for SPIDER, 7.4 fs for SH-FROG, and 6.8 fs for FM-FROG.

same dispersion in the beam path, including beam splitter dispersion and air paths. The result of the SPIDER measurement is quite reassuring, reproducing the pulse duration of FM-FROG and the satellite structure on small delays very well, compare Fig. 6(a) and Figs. 6(c,e). The global shape of the spectral phase measured by all three methods is also virtually identical and deviates only for vanishing spectral intensity [Figs. 6(b,d,e)]. FROG does not reproduce some of the fine-structure in the SPIDER measurement, which is not a surprise, as FROG has to indirectly retrieve this small ripple, whereas SPIDER directly measures it.

As the SH-FROG trace has to be extracted from the IFROG trace with background subtraction, its dynamic range is not overly high, leading to larger values of the FROG error than with background-free methods. Consequently, the retrieved pulse with a FWHM duration of 7.4 fs and its spectrum [Fig. 6(c,d)] differ more strongly from the SPIDER measurement and marginal test than the results retrieved from FM-FROG [Fig. 6(e,f)]. The reconstructed spectral density from the FM-FROG retrieval [Fig. 6(f)] differs only in some small detail from the measured one [Fig. 6(b)]. For example, the central highly modulated part of the spectrum appears averaged in the FM-FROG spectrum, which is due to gridding of the trace. Also, small deviations in the far wings of the spectrum are related to the intensity correction of the IFROG trace. Otherwise the agreement is excellent.

In conclusion, we found that SH-FROG extraction works fairly well for an interferometric collinear FROG geometry, but has its apparent weaknesses, which are clearly resolvable in the comparison of the reconstructed pulse shapes and spectra. Retrieval from the modulational part requires fringe integrity, but pays off in a much better reconstruction of the pulse shape. Combination of both approaches is extremely helpful. Standard SH-FROG uses proven retrieval

#6789 - $15.00 US
Received 8 March 2005; revised 22 March 2005; accepted 22 March 2005
(C) 2005 OSA

algorithms that deliver rapid convergence to an approximate solution. So far, we only applied a modified GPA method to reconstruct the pulse shape from the FM-FROG data. It is generally known, that these algorithms work very well when seeded with an approximate solution. Nevertheless, they are slow in producing early convergence. Therefore a combination of both methods as described appears to be ideal for rapid and precise determination of pulse shapes from an IFROG trace. It should be pointed out that all three approaches yield approximately the same results in terms of pulse duration. In particular, SPIDER (6.5 fs) and FM-FROG (6.8 fs) gave an excellent agreement.

6. Conclusion

In conclusion, we presented a novel approach to FROG characterization in the few-cycle regime. Being based on interferometric autocorrelation, the setup is considerably simpler to align than a noncollinear FROG. No careful optimization of the crossing angle is required to keep geometrical blurring at a minimum. In terms of data acquisition, this technique is more challenging, as it requires rapid acquisition of the spectra to avoid corruption of the data by interferometer drift. As a benefit of this higher complexity, IFROG does not only deliver an unblurred standard FROG trace, but also provides valuable additional information in the interferometric modulation: a background-free FM-FROG trace. Other than standard FROG methods, which are sensitive only to the temporal and spectral shape of the pulse, the FM trace exhibits some direct phase sensitivity and is directly affected by a linear chirp. A comparison to an independent SPIDER measurement confirms the reliability of this new pulse characterization method. Interferometric FROG is the straightforward extension of interferometric autocorrelation, which has long been the method of choice for measuring sub-10-fs pulses. Existing interferometric autocorrelators can easily be upgraded for measurement of the IFROG trace. With the added cross-checks, interferometric FROG significantly increases the number of choices for few-cycle pulse measurements.

#6789 - $15.00 US Received 8 March 2005; revised 22 March 2005; accepted 22 March 2005
(C) 2005 OSA